arXiv:hep-ex/0201014v2 9 Jan 2002

EUROPEAN ORGANIZATION FOR NUCLEAR RESEARCH (CERN)
European Laboratory for Particle Physics

CERN-EP/2001-095
18-Dec-2001

Final results of the searches for neutral Higgs bosons in e^+e^- collisions at $\sqrt{s}$ up to 209 GeV

The ALEPH Collaboration *)

Abstract

The final results of the ALEPH search for the Standard Model Higgs boson at LEP, with data collected in the year 2000 at centre-of-mass energies up to 209 GeV, are presented. The changes with respect to the preceding publication are described and a complete study of systematic effects is reported. The findings of this final analysis confirm the preliminary results published in November 2000 shortly after the closing down of the LEP collider: a significant excess of events is observed, consistent with the production of a 115 GeV/c^2 Standard Model Higgs boson. The final results of the searches for the neutral Higgs bosons of the MSSM are also reported, in terms of limits on m_{h}, m_{A} and $\tan\beta$. Limits are also set on m_{h} in the case of invisible decays.

To be published in Physics Letters B

*) See next pages for the list of authors.

The ALEPH Collaboration

A. Heister, S. Schael

Physikalisches Institut das RWTH-Aachen, D-52056 Aachen, Germany

R. Barate, R. Brunelière, I. De Bonis, D. Decamp, C. Goy, S. Jezequel, J.-P. Lees, F. Martin, E. Merle, M.-N. Minard, B. Pietrzyk, B. Trocmé

Laboratoire de Physique des Particules (LAPP), IN^{2}P^3-CNRS, F-74019 Annecy-le-Vieux Cedex, France

G. Boix, S. Bravo, M.P. Casado, M. Chmeissani, J.M. Crespo, E. Fernandez, M. Fernandez-Bosman, Ll. Garrido,[15] E. Graugés, J. Lopez, M. Martinez, G. Merino, R. Miquel,[31] Ll.M. Mir,[31] A. Pacheco, D. Paneque, H. Ruiz

Institut de Física d'Altes Energies, Universitat Autònoma de Barcelona, E-08193 Bellaterra (Barcelona), Spain[7]

A. Colaleo, D. Creanza, N. De Filippis, M. de Palma, G. Iaselli, G. Maggi, M. Maggi, S. Nuzzo, A. Ranieri, G. Raso,[24] F. Ruggieri, G. Selvaggi, L. Silvestris, P. Tempesta, A. Tricomi,[3] G. Zito

Dipartimento di Fisica, INFN Sezione di Bari, I-70126 Bari, Italy

X. Huang, J. Lin, Q. Ouyang, T. Wang, Y. Xie, R. Xu, S. Xue, J. Zhang, L. Zhang, W. Zhao

Institute of High Energy Physics, Academia Sinica, Beijing, The People's Republic of China[8]

D. Abbaneo, P. Azzurri, T. Barklow,[30] O. Buchmüller,[30] M. Cattaneo, F. Cerutti, B. Clerbaux, H. Drevermann, R.W. Forty, M. Frank, F. Gianotti, T.C. Greening,[26] J.B. Hansen, J. Harvey, D.E. Hutchcroft, P. Janot, B. Jost, M. Kado,[31] P. Maley, P. Mato, A. Moutoussi, F. Ranjard, L. Rolandi, D. Schlatter, G. Sguazzoni, W. Tejessy, F. Teubert, A. Valassi, I. Videau, J.J. Ward

European Laboratory for Particle Physics (CERN), CH-1211 Geneva 23, Switzerland

F. Badaud, S. Dessagne, A. Falvard,[20] D. Fayolle, P. Gay, J. Jousset, B. Michel, S. Monteil, D. Pallin, J.M. Pascolo, P. Perret

Laboratoire de Physique Corpusculaire, Université Blaise Pascal, IN^{2}P^3-CNRS, Clermont-Ferrand, F-63177 Aubière, France

J.D. Hansen, J.R. Hansen, P.H. Hansen, B.S. Nilsson, A. Wäänänen

Niels Bohr Institute, 2100 Copenhagen, DK-Denmark[9]

A. Kyriakis, C. Markou, E. Simopoulou, A. Vayaki, K. Zachariadou

Nuclear Research Center Demokritos (NRCD), GR-15310 Attiki, Greece

A. Blondel,[12] J.-C. Brient, F. Machefert, A. Rougé, M. Swynghedauw, R. Tanaka H. Videau

Laboratoire de Physique Nucléaire et des Hautes Energies, Ecole Polytechnique, IN^{2}P^3-CNRS, F-91128 Palaiseau Cedex, France

V. Ciulli, E. Focardi, G. Parrini

Dipartimento di Fisica, Università di Firenze, INFN Sezione di Firenze, I-50125 Firenze, Italy

A. Antonelli, M. Antonelli, G. Bencivenni, G. Bologna,[4] F. Bossi, P. Campana, G. Capon, V. Chiarella, P. Laurelli, G. Mannocchi,[5] F. Murtas, G.P. Murtas, L. Passalacqua, M. Pepe-Altarelli,[25] P. Spagnolo

Laboratori Nazionali dell'INFN (LNF-INFN), I-00044 Frascati, Italy

J. Kennedy, J.G. Lynch, P. Negus, V. O'Shea, D. Smith, A.S. Thompson

Department of Physics and Astronomy, University of Glasgow, Glasgow G12 8QQ,United Kingdom[10]

S. Wasserbaech

Department of Physics, Haverford College, Haverford, PA 19041-1392, U.S.A.

R. Cavanaugh, S. Dhamotharan, C. Geweniger, P. Hanke, V. Hepp, E.E. Kluge, G. Leibenguth, A. Putzer, H. Stenzel, K. Tittel, S. Werner,[19] M. Wunsch[19]

Kirchhoff-Institut für Physik, Universität Heidelberg, D-69120 Heidelberg, Germany[16]

R. Beuselinck, D.M. Binnie, W. Cameron, G. Davies, P.J. Dornan, M. Girone,[1] R.D. Hill, N. Marinelli, J. Nowell, H. Przysiezniak,[2] S.A. Rutherford, J.K. Sedgbeer, J.C. Thompson,[14] R. White

Department of Physics, Imperial College, London SW7 2BZ, United Kingdom[10]

V.M. Ghete, P. Girtler, E. Kneringer, D. Kuhn, G. Rudolph

Institut für Experimentalphysik, Universität Innsbruck, A-6020 Innsbruck, Austria[18]

E. Bouhova-Thacker, C.K. Bowdery, D.P. Clarke, G. Ellis, A.J. Finch, F. Foster, G. Hughes, R.W.L. Jones, M.R. Pearson, N.A. Robertson, M. Smizanska

Department of Physics, University of Lancaster, Lancaster LA1 4YB, United Kingdom[10]

V. Lemaitre

Institut de Physique Nucléaire, Département de Physique, Université Catholique de Louvain, 1348 Louvain-la-Neuve, Belgium

U. Blumenschein, F. Hölldorfer, K. Jakobs, F. Kayser, K. Kleinknecgt, A.-S. Müller, G. Quast,[6] B. Renk, H.-G. Sander, S. Schmeling, H. Wachsmuth, C. Zeitnitz, T. Ziegler

Institut für Physik, Universität Mainz, D-55099 Mainz, Germany[16]

A. Bonissent, J. Carr, P. Coyle, C. Curtil, A. Ealet, D. Fouchez, O. Leroy, T. Kachelhoffer, P. Payre, D. Rousseau, A. Tilquin

Centre de Physique des Particules de Marseille, Univ Méditerranée, IN^{2}P^3-CNRS, F-13288 Marseille, France

F. Ragusa

Dipartimento di Fisica, Università di Milano e INFN Sezione di Milano, I-20133 Milano, Italy.

A. David, H. Dietl, G. Ganis,[27] K. Hüttmann, G. Lütjens, C. Mannert, W. Männer, H.-G. Moser, R. Settles, G. Wolf

Max-Planck-Institut für Physik, Werner-Heisenberg-Institut, D-80805 München, Germany[16]

J. Boucrot, O. Callot, M. Davier, L. Duflot, J.-F. Grivaz, Ph. Heusse, A. Jacholkowska,[20] C. Loomis, L. Serin, J.-J. Veillet, J.-B. de Vivie de Régie,[28] C. Yuan

Laboratoire de l'Accélérateur Linéaire, Université de Paris-Sud, IN^{2}P^3-CNRS, F-91898 Orsay Cedex, France

G. Bagliesi, T. Boccali, L. Foà, A. Giammanco, A. Giassi, F. Ligabue, A. Messineo, F. Palla, G. Sanguinetti, A. Sciabà, R. Tenchini,[1] A. Venturi,[1] P.G. Verdini

Dipartimento di Fisica dell'Università, INFN Sezione di Pisa, e Scuola Normale Superiore, I-56010 Pisa, Italy

O. Awunor, G.A. Blair, J. Coles, G. Cowan, A. Garcia-Bellido, M.G. Green, L.T. Jones, T. Medcalf, A. Misiejuk, J.A. Strong, P. Teixeira-Dias

Department of Physics, Royal Holloway & Bedford New College, University of London, Egham, Surrey TW20 OEX, United Kingdom[10]

R.W. Clifft, T.R. Edgecock, P.R. Norton, I.R. Tomalin

Particle Physics Dept., Rutherford Appleton Laboratory, Chilton, Didcot, Oxon OX11 OQX, United Kingdom[10]

B. Bloch-Devaux, D. Boumediene, P. Colas, B. Fabbro, E. Lançon, M.-C. Lemaire, E. Locci, P. Perez, J. Rander, J.-F. Renardy, A. Rosowsky, P. Seager,[13] A. Trabelsi,[21] B. Tuchming, B. Vallage

CEA, DAPNIA/Service de Physique des Particules, CE-Saclay, F-91191 Gif-sur-Yvette Cedex, France[17]

N. Konstantinidis, A.M. Litke, G. Taylor

Institute for Particle Physics, University of California at Santa Cruz, Santa Cruz, CA 95064, USA[22]

C.N. Booth, S. Cartwright, F. Combley,[4] P.N. Hodgson, M. Lehto, L.F. Thompson

Department of Physics, University of Sheffield, Sheffield S3 7RH, United Kingdom[10]

K. Affholderbach,[23] A. Böhrer, S. Brandt, C. Grupen, J. Hess, A. Ngac, G. Prange, U. Sieler

Fachbereich Physik, Universität Siegen, D-57068 Siegen, Germany[16]

C. Borean, G. Giannini

Dipartimento di Fisica, Università di Trieste e INFN Sezione di Trieste, I-34127 Trieste, Italy

H. He, J. Putz, J. Rothberg

Experimental Elementary Particle Physics, University of Washington, Seattle, WA 98195 U.S.A.

S.R. Armstrong, K. Berkelman, K. Cranmer, D.P.S. Ferguson, Y. Gao,[29] S. González, O.J. Hayes, H. Hu, S. Jin, J. Kile, P.A. McNamara III, J. Nielsen, Y.B. Pan, J.H. von Wimmersperg-Toeller, W. Wiedenmann, J. Wu, Sau Lan Wu, X. Wu, G. Zobernig

Department of Physics, University of Wisconsin, Madison, WI 53706, USA[11]

G. Dissertori

Institute for Particle Physics, ETH Hönggerberg, 8093 Zürich, Switzerland.

---

[1]Also at CERN, 1211 Geneva 23, Switzerland.

[2]Now at LAPP, 74019 Annecy-le-Vieux, France

[3]Also at Dipartimento di Fisica di Catania and INFN Sezione di Catania, 95129 Catania, Italy.

[4]Deceased.

[5]Also Istituto di Cosmo-Geofisica del C.N.R., Torino, Italy.

[6]Now at Institut für Experimentelle Kernphysik, Universität Karlsruhe, 76128 Karlsruhe, Germany.

[7]Supported by CICYT, Spain.

[8]Supported by the National Science Foundation of China.

[9]Supported by the Danish Natural Science Research Council.

[10]Supported by the UK Particle Physics and Astronomy Research Council.

[11]Supported by the US Department of Energy, grant DE-FG0295-ER40896.

[12]Now at Departement de Physique Corpusculaire, Université de Genève, 1211 Genève 4, Switzerland.

[13]Supported by the Commission of the European Communities, contract ERBFMBICT982874.

[14]Also at Rutherford Appleton Laboratory, Chilton, Didcot, UK.

[15]Permanent address: Universitat de Barcelona, 08208 Barcelona, Spain.

[16]Supported by the Bundesministerium für Bildung, Wissenschaft, Forschung und Technologie, Germany.

[17]Supported by the Direction des Sciences de la Matière, C.E.A.

[18]Supported by the Austrian Ministry for Science and Transport.

[19]Now at SAP AG, 69185 Walldorf, Germany

[20]Now at Groupe d' Astroparticules de Montpellier, Université de Montpellier II, 34095 Montpellier, France.

[21]Now at Département de Physique, Faculté des Sciences de Tunis, 1060 Le Belvédère, Tunisia.

[22]Supported by the US Department of Energy, grant DE-FG03-92ER40689.

[23]Now at Skyguide, Swissair Navigation Services, Geneva, Switzerland.

[24]Also at Dipartimento di Fisica e Tecnologie Relative, Università di Palermo, Palermo, Italy.

[25]Now at CERN, 1211 Geneva 23, Switzerland.

[26]Now at Honeywell, Phoenix AZ, U.S.A.

[27]Now at INFN Sezione di Roma II, Dipartimento di Fisica, Università di Roma Tor Vergata, 00133 Roma, Italy.

[28]Now at Centre de Physique des Particules de Marseille, Univ Méditerranée, F-13288 Marseille, France.

[29]Also at Department of Physics, Tsinghua University, Beijing, The People's Republic of China.

[30]Now at SLAC, Stanford, CA 94309, U.S.A.

1 Introduction

In November 2000, ten days after the closing down of the LEP collider, the ALEPH collaboration published the preliminary findings [1] of their search for the Standard Model (SM) Higgs boson [2]. An excess of events was found in the data collected in the year 2000 at centre-of-mass energies up to 209 GeV, in agreement with the production of a 114–115 GeV/c^2 SM Higgs boson. The probability that this excess is consistent with the background-only hypothesis was determined to be at the level of a few permil, corresponding to a $\sim 3\sigma$ effect. The other three LEP experiments have also reported their search results [3, 4, 5].

In this letter, after a brief reminder in Section 2 of the overall analysis methodology, the changes with respect to the preliminary analysis presented in Ref. [1] are described. These minor modifications mostly affect the four-jet channel $\mathrm{hq\bar{q}}$, arising from the $\mathrm{e^+e^-}\rightarrow \mathrm{hZ}$ Higgsstrahlung process with subsequent hadronic decays of the Higgs and Z bosons, in which the three highest-purity events were selected. They also affect, although to a lesser extent, the other three main topologies, i.e., the missing energy channel $\mathrm{h}\nu\bar{\nu}$, the leptonic channel $\mathrm{h}\ell^+\ell^-$, where ℓ is either an electron or a muon, and the final states with taus $\tau^+\tau^-\mathrm{q\bar{q}}$, when either the Higgs or the Z boson decays to $\tau^+\tau^-$.

The final updates to the analysis, described in Section 3 together with their effect on the result, are fourfold:

- the data sample was reprocessed with the final detector calibration and alignment constants for the year 2000;
- the precise knowledge of the LEP centre-of-mass energy was propagated to the final results;
- additional simulated event samples were produced for a statistically more accurate prediction of the Standard Model backgrounds;
- an algorithm was developed to reject beam-related backgrounds and was applied in the four-jet channel.

The results of the final combination of the searches for the Standard Model Higgs boson, with these updates included, are given in Section 4, followed by a complete discussion of the systematic uncertainties in Section 5. Other relevant details of the analysis can be found in Ref. [1].

The search for the $\mathrm{b\bar{b}b\bar{b}}$ and $\mathrm{b\bar{b}}\tau^+\tau^-$ final states, which may arise from the associated production $\mathrm{e^+e^-}\rightarrow \mathrm{hA}$ in two-Higgs doublet models, was also updated in the framework of the Minimal Supersymmetric extension of the Standard Model (MSSM) with the data collected in the year 2000. The final combination of the hZ and hA searches with the results obtained at lower energies [6, 7] is presented in Section 6.

Finally, possible invisible decays of a Higgs boson produced via the Higgsstrahlung process were investigated with the data collected in the year 2000. The result of the combination with earlier searches [7, 8] is reported in Section 7.

2 Search methodology

In order to provide mutually cross-checked results, the Higgs boson search is carried out in two alternative "streams", the first relying mostly on neural networks (NN) for the event selections, and the second on sequential cuts. The final results are those obtained in the NN stream. In the hZ search, the two streams differ in the treatment of the two most powerful search channels: the four-jet and the missing energy final states. The treatment of the $\mathrm{h}\ell^+\ell^-$ and $\tau^+\tau^-\mathrm{q\bar{q}}$ channels is identical in the two streams. The defining characteristics of the cut stream and of the NN stream are summarized in Table 1.

The event selection criteria of the different search channels, used for the analysis of the 2000 data [1], are very similar to those used for the 1999 data [7]. For the results presented in this letter the event selections are identical to those of Ref. [1], with only one improvement (described in detail in Section 3.4) made to the four-jet selection.

In each search channel the likelihood of a signal in the data is quantified by means of an extended likelihood ratio Q [9]

$$Q = \frac{L_{s+b}}{L_b} = \frac{e^{-(s+b)}}{e^{-b}} \prod_{i=1}^{n_{\mathrm{obs}}} \frac{s f_s(\vec{X}_i) + b f_b(\vec{X}_i)}{b f_b(\vec{X}_i)},$$

which combines information about the numbers of events observed (n_{obs}) and expected in both the background-only (b) and the signal ($s + b$) hypotheses. It also contains information, through the signal and background probability density functions (pdf's) f_s and f_b, that provides additional discrimination between the two hypotheses. The pdf's are evaluated for each observed candidate i, with measured discriminant variables $\vec{X}_i$. The discriminant variable(s) used in each search channel of the two analysis streams are listed in Table 1. The likelihood ratio for the combined search is the product of the likelihood ratios of the individual search channels.

Table 1: The main features of the two analysis streams. For each search channel ($\mathrm{hq\bar{q}}$, $\mathrm{h}\nu\bar{\nu}$, etc.) the type of event selection ("Cuts" or "NN") is indicated. The observables X denote the discriminant variables used for the calculation of the likelihood ratio: M_{rec} denotes generically the reconstructed mass, as defined for the given channel [1], and $\mathrm{NN_{output}}$ refers to the output of the NN used for the event selection.

	Cut stream		NN stream	
Search channel	Event selection	Discriminant variable(s)	Event selection	Discriminant variable(s)
$\mathrm{hq\bar{q}}$	Cuts	$X = M_{\mathrm{rec}}$	NN	$\vec{X} = (M_{\mathrm{rec}}, \mathrm{NN_{output}})$
$\mathrm{h}\nu\bar{\nu}$	Cuts	$X = M_{\mathrm{rec}}$	NN	$\vec{X} = (M_{\mathrm{rec}}, \mathrm{b_{tag}})$
$\mathrm{h}\ell^+\ell^-$	Cuts	$\vec{X} = (M_{\mathrm{rec}}, \mathrm{b}\tau_{\mathrm{tag}})$	Cuts	$\vec{X} = (M_{\mathrm{rec}}, \mathrm{b}\tau_{\mathrm{tag}})$
$\tau^+\tau^-\mathrm{q\bar{q}}$	NN	$X = M_{\mathrm{rec}}$	NN	$X = M_{\mathrm{rec}}$

The cut stream uses mostly the reconstructed mass M_{rec} [1] as a single discriminant. The exception is the $\mathrm{h}\ell^+\ell^-$ channel: in this case, as the event selection has no b-tagging cuts, the inclusion of the second discriminant (to tag b and τ jets) is necessary.

3 Analysis updates

The updates made to the analysis of Ref. [1], mentioned in Section 1, are described in detail in the following subsections. The effect of each of these updates on the significance of the observed excess [1] is displayed in Table 2. The properties of the most significant four-jet candidates, after all the analysis updates are taken into account, are listed in Table 3.

Table 2: The successive effect of the analysis changes on the maximum significance of the observed excess, for the two alternative analysis streams.

Update	Cut stream	NN stream
Significance [1]	3.06σ	2.96σ
Final processing	$+0.21\sigma$	-0.14σ
LEP $\sqrt{s}$	–	–
Additional simulated event samples	-0.36σ	-0.14σ
Beam-background	$+0.13\sigma$	$+0.14\sigma$
Final significance	3.04σ	2.82σ

Table 3: Details of the five four-jet candidates selected with an event weight greater than 0.3 at $m_{\mathrm{h}} = 115\,\mathrm{GeV}/c^2$ in either the NN or cut streams. Jets 3 and 4 are the Higgs boson jets. The weight $w = \ln(1 + sf_s/bf_b)$ of the candidates in each stream is also given. For candidate e, the jet pairing shown is only selected in the cut stream.

Candidate (Run/Event)	M_{rec} (GeV/c^2)	b tagging				Four-jet NN	w_{NN}	w_{cut}
		Jet 1	Jet 2	Jet 3	Jet 4			
a (56698/7455)	109.9	0.999	0.831	0.999	0.197	0.999	0.59	0.25
b (56065/3253)	114.4	0.996	0.663	1.000	0.996	0.997	1.44	0.81
c (54698/4881)	114.1	0.124	0.012	0.998	0.999	0.997	1.76	0.61
d (56366/0955)	114.4	0.201	0.051	0.998	0.956	0.933	0.41	0.62
e (55982/6125)	114.4	0.071	0.306	0.449	0.998	0.687	–	0.63

3.1 Final processing

The data were reprocessed with the final detector calibration and alignment constants. This reprocessing resulted in the recovery of $1\,\mathrm{pb}^{-1}$ of data. The total integrated luminosity for the year 2000 is $\mathcal{L} = 217.2\,\mathrm{pb}^{-1}$.

The reprocessing can change by small amounts the value of measured event properties such as the reconstructed Higgs boson mass or the b-tagging probabilities. Events close to some of the selection cuts may therefore move into or out of the selected sample. About 95% of the data events selected previously were also selected after the final processing. More specifically, the most signal-like events, i.e., those with a large contribution to the log-likelihood ratio $-2\ln Q$, are still selected after the final processing.

In the cut-based four-jet channel, a new event is selected with a reconstructed Higgs boson mass of $111.8\,\mathrm{GeV}/c^2$. Prior to the reprocessing, this event narrowly failed one

of the b-tagging cuts. The two Higgs-candidate jets have b-tagging values of 0.870 and 0.965, whereas the Z-candidate jets have b-tag values of 0.096 and 0.277. (The output of the neural network b-tagging algorithm ranges from 0. for light-quark jets, to 1. for b-quark jets.) The missing energy of the event is 70 GeV and the total missing momentum is below $10\,\mathrm{GeV}/c$. A probable explanation for the large missing energy and low missing momentum is that two energetic neutrinos were produced almost back to back by two b-quark semileptonic decays. Indeed, in one of the b-tagged jets, an identified muon has a momentum of $1.7\,\mathrm{GeV}/c$ transverse to the jet axis and is therefore consistent with a semileptonic decay of a b hadron. Another low-momentum muon is observed opposite to this jet, which further substantiates this hypothesis.

In the cut stream, where only the reconstructed mass information is used as a discriminant, the event is assigned a weight $\ln(1 + sf_s/bf_b) = 0.27$ at $m_{\mathrm{h}} = 115\,\mathrm{GeV}/c^2$. In the NN stream, this event was already selected prior to the final processing. The event has a NN output of 0.90, and is therefore assigned a relatively low weight compared to the most significant candidates [1].

3.2 LEP centre-of-mass energy

In the most recently available determination [10], the centre-of-mass energies are, on average, smaller than those used in Ref. [1] by $\sim 140\,\mathrm{MeV}$. When this effect is taken into account, the reconstructed Higgs boson masses of the candidate events are reduced by the same amount, and the number of signal events expected to be produced decreases from 10.1 to 9.5 for $m_{\mathrm{h}} = 115\,\mathrm{GeV}/c^2$. The impact on the observed significance is negligible.

3.3 Additional simulated event samples

In order to further reduce the statistical uncertainty in the event selection efficiencies and in the pdf's, significantly larger event samples were generated. In particular, additional simulated background samples for the $\mathrm{e^+e^-} \to \mathrm{b\bar{b}}(\gamma), \mathrm{c\bar{c}}(\gamma), \mathrm{W^+W^-}$ and ZZ processes were generated at centre-of-mass energies $\sqrt{s}$ = 206.0, 206.7 and 207.0 GeV. The existing signal samples were also supplemented with samples of $\mathrm{e^+e^-} \to \mathrm{hq\bar{q}}$ and $\mathrm{h}\nu\bar{\nu}$ events at $\sqrt{s} = 206.7$ GeV. While most of these additional samples were used in the NN stream for the preliminary results [1], they have only been included in the cut stream for this letter.

3.4 Control of beam-induced backgrounds

In one of the most significant four-jet events, called "candidate *b*" in Table 3, a 22 GeV energy deposit is observed at small polar angle, in the plane of the collider.

This deposit does not fit the hypothesis that it is part of the event. The total measured energy is considerably larger than $\sqrt{s}$ and the total measured momentum is aligned with that of the deposit. A reasonable kinematic fit quality is obtained only if this deposit is assumed to be extraneous to the event, i.e., produced by a beam-induced background particle.

It is indeed possible to observe large energy clusters from this background source. For example, in 0.89% (0.48%) of events triggered at random beam crossings, a deposit of

energy in excess of 3 (10) GeV is observed. The angular position of the most energetic cluster observed within 12° of the beam axis, in the randomly-triggered event sample, is shown in Fig. 1a. The overwhelming majority of the beam-induced background particles are at very small polar angles and in the plane of the collider.

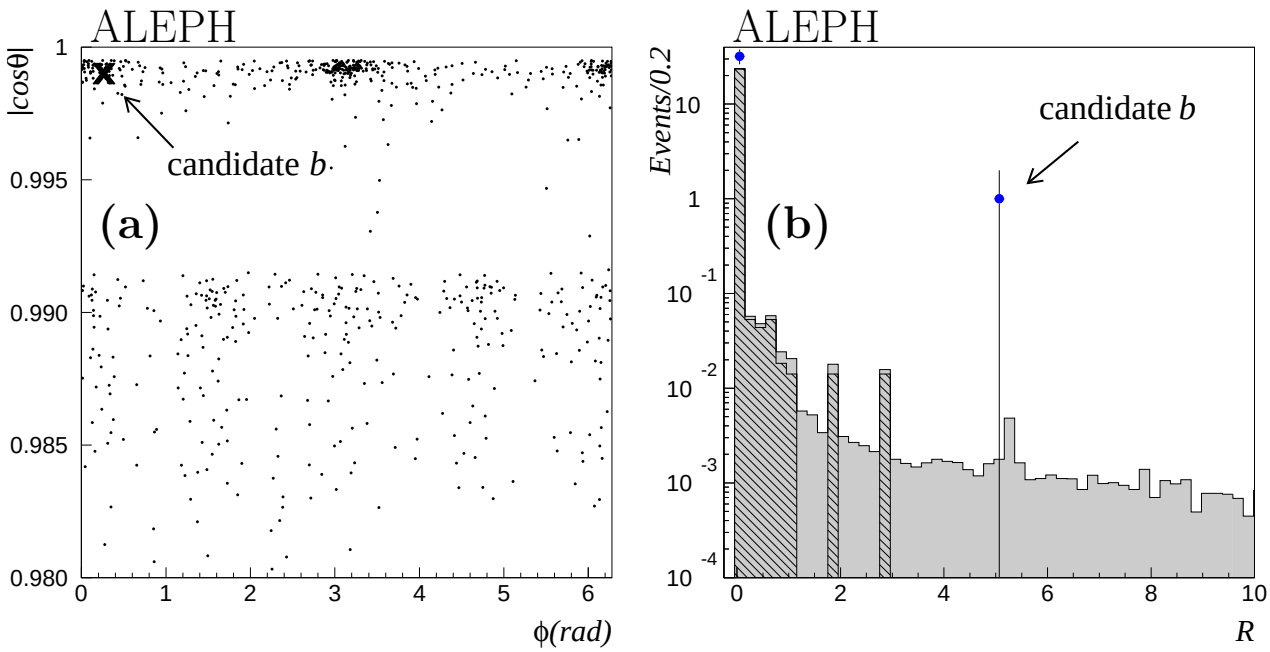

Figure 1: (a) The angular distribution of the most energetic cluster observed within 12° of the beam axis, in a sample of events from randomly-triggered beam crossings. Only clusters with $E > 3$ GeV are shown. The candidate event b is indicated by the cross in the upper-left corner. The plane of the collider is defined by $\phi = 0$ and π. (b) The distribution of R for the events selected by the cut-based four-jet search, for the expected SM background with (shaded histogram) and without (hatched histogram) contamination from beam-related background, and for the data (dots with error bars).

As this type of background is not simulated, a procedure to identify and remove beam-background clusters had to be developed. The most energetic cluster with energy greater than 3 GeV, $|\cos\theta| > 0.998$ and which is isolated by at least 8° with respect to any other particle in the event, is fitted to each of the following three hypotheses.

- The identified cluster is part of the event. In this case, the identified cluster is assigned to one of the four jets by the jet clustering procedure. The jets are subsequently fitted to the total energy- and momentum-conservation constraints.

- The identified cluster is, more specifically, assumed to be an ISR photon. In this case, the rest of the event is forced to form four jets. These jets are fitted to the total energy- and momentum-conservation constraints, modified to account for the momentum imbalance caused by the hypothetical ISR photon.

- The identified cluster is assumed to originate from a beam-induced background particle. In this case too, the rest of the event is forced to form four jets. These jets are subsequently fitted to the total energy- and momentum-conservation constraints.

The χ^2 values of these fits are henceforth designated $\chi^2_{\rm norm}, \chi^2_{\rm ISR}$ and $\chi^2_{\rm beam}$, respectively. The ratio

$$R = \frac{\min(\chi^2_{\rm norm}, \chi^2_{\rm ISR})}{\chi^2_{\rm beam}}$$

is expected to be larger for events containing a beam-background particle. The distribution of R for the total expected SM background is shown in Fig. 1b, before and after it is "contaminated" with beam-background clusters obtained from a sample of randomly-triggered events. Events in which no energetic, isolated, small-angle cluster is found are assigned $R = 0$. Events with $R > 2.$ are tagged as containing a beam-background particle and the identified cluster of energy is removed from the event prior to jet clustering and kinematic fitting. The remaining events are treated according to the first hypothesis.

The efficiency of the beam-background cleaning procedure, determined by running the algorithm on a contaminated background sample, is 28% (50%) for events with energy deposits in excess of 3 GeV (10 GeV). The purity of the identification procedure is close to 100%.

At the final selection level 1.2% of the simulated events are affected (i.e., newly selected, no longer selected, or with an $M_{\rm rec}$ value changed by at least $1\,{\rm GeV}/c^2$) by the contamination. This fraction is reduced to 0.4% after the cleaning procedure is applied. The corresponding changes to the selection efficiencies are statistically insignificant and the changes in the pdf's imperceptible.

When applied to the data, the cleaning algorithm identifies only one event (candidate b) as containing a beam-induced energy deposit. The deposit is therefore ignored in the analysis of this event, and the reconstructed Higgs mass (neural network output) changes from $112.8\,{\rm GeV}/c^2$ (0.996) to $114.4\,{\rm GeV}/c^2$ (0.997).

4 Results of the SM Higgs search

In the $217.2\,{\rm pb}^{-1}$ of data collected during the year 2000, 137 (99) events were selected in the NN (cut) stream, with 129.9 (88.2) expected from Standard Model backgrounds. The distribution of the events among the four search channels is shown in Table 4. The mass distributions are very similar to those of Ref. [1].

The log-likelihood ratio, shown in Fig. 2a as a function of the test mass $m_{\rm h}$, includes the data collected at smaller centre-of-mass energies [6, 7]. The large negative values of the observed log-likelihood ratio indicate that the data favour the signal hypothesis over the background-only hypothesis. The most likely Higgs boson mass, corresponding to the minimum of $-2\ln Q$, is around $m_{\rm h} = 115\,{\rm GeV}/c^2$ for the NN stream. At this mass the likelihood for the signal hypothesis, L_{s+b}, is 28.6 times larger than the likelihood of the background-only hypothesis, L_b. In the cut stream a similar result is observed (Fig. 2b), with a preferred signal mass closer to $m_{\rm h} = 114.5\,{\rm GeV}/c^2$ and a factor 21.9 between the likelihoods of the two hypotheses. The probability (denoted $1-c_{\rm b}$) that this ratio be even larger than observed in the background-only hypothesis is shown in Fig. 4 as a function of $m_{\rm h}$. At the minimum of $1-c_{\rm b}$, this probability is 2.4×10^{-3} (1.1×10^{-3}) in the NN (cut)

Table 4: The expected numbers of signal and background events and the numbers of observed candidates in each search channel, for the two analysis streams ("NN" and "Cut"). The signal expectation is determined at $m_{\mathrm{h}} = 115\,\mathrm{GeV}/c^2$.

Search channel	Signal expected	Background expected	Events observed
$\mathrm{hq\bar{q}}$ (NN)	3.0	47.7	53
$\mathrm{hq\bar{q}}$ (cut)	1.8	23.9	33
$\mathrm{h}\nu\bar{\nu}$ (NN)	1.0	37.7	39
$\mathrm{h}\nu\bar{\nu}$ (cut)	0.9	19.8	21
$\mathrm{h}\ell^+\ell^-$	0.4	30.8	30
$\tau^+\tau^-\mathrm{q\bar{q}}$	0.3	13.7	15
NN stream total	4.7	129.9	137
Cut stream total	3.4	88.2	99

stream, corresponding to an excess of 2.82 (3.04) standard deviations[1]. At the minimum of the likelihood ratio, the significance of the excess is 2.70 (2.87) standard deviations. It is consistent with the signal expectation at the 1.06 (1.29) standard deviations level.

Due to the observed excess, the 95% C.L. lower limit of $111.5\,\mathrm{GeV}/c^2$ set on m_{h} in the NN stream search is well below the limit of $114.2\,\mathrm{GeV}/c^2$ expected in the absence of a signal. For comparison, a lower limit of $110.4\,\mathrm{GeV}/c^2$ is set in the cut stream, with $113.6\,\mathrm{GeV}/c^2$ expected.

5 Systematic uncertainties

The results given in Section 4 include systematic uncertainties, incorporated according to the method of Ref. [12]. However, the significance of the excess might be affected by systematic uncertainties in a different manner. The systematic studies were therefore extended to estimate the impact of the dominant sources on the measured confidence levels (Fig. 3), especially around $m_{\mathrm{h}} = 116\,\mathrm{GeV}/c^2$, where $1 - c_b$ is smallest. The uncertainties in the $\mathrm{h}\nu\bar{\nu}$ channel were found to be negligible. The different systematic uncertainty sources and their impact on the observed significance are summarized in Table 5 and are discussed below. The uncertainties on the background dominate over those on the signal.

1. **Statistics of simulated samples**
   To a large extent, the separation power between the background-only and the signal hypotheses comes from the inclusion of the discriminant variable pdf's in the likelihood ratio definition. It is especially so for a signal close to threshold, for which the event rate is low. The statistical uncertainty on the pdf's, which arises

[1]The LEP Higgs working group [11] has adopted a different convention, using a double-sided Gaussian, to convert probability into standard deviations. Under that convention the significance of the excess is 3.04 standard deviations in the NN stream and 3.25 standard deviations in the cut stream.

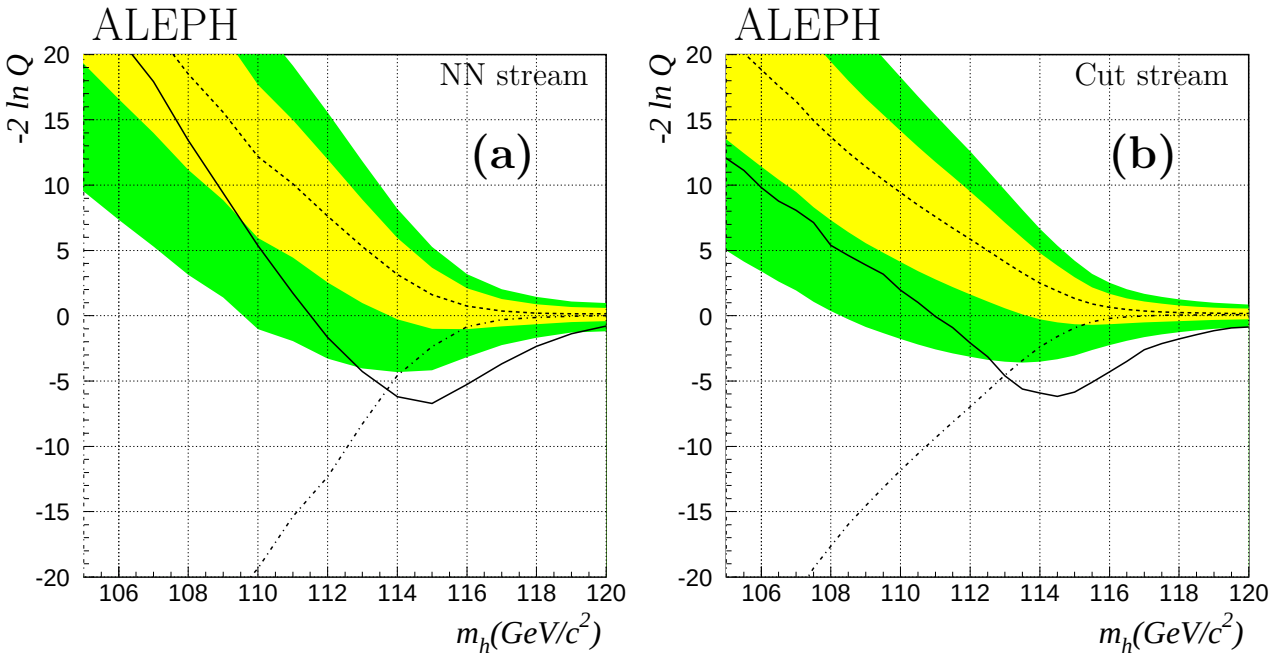

Figure 2: The log-likelihood ratio, $-2\ln Q$, as a function of the test mass m_{h} for (a) the NN stream and (b) the cut stream, with all data taken from 189 - 209 GeV. The solid line is the result obtained from the data. The average result of background-only simulated experiments is indicated by the dashed line; the light and dark shaded bands around the background expectation contain 68% and 95% of the simulated background-only experiments, respectively. The dash-dotted curves indicate the expected position of the median log-likelihood when the latter is calculated at a mass m_{h} and includes a signal at that same mass.

from the finite statistics of the simulated samples, may therefore have an important impact on the significance of the observed excess.

The small correlation between the two discriminant variables of the NN-based four-jet search, ignored in the pdf's, was propagated to the observed significance. The resulting correction is small, and its uncertainty is limited by the finite statistics of the simulated samples. The systematic uncertainty on the correction is estimated to be half the size of the correction.

In the remaining search channels, the systematic uncertainty due to the limited size of the simulated samples was determined by comparing pdf's fitted to statistically independent samples of simulated events. For instance, in the cut-based four-jet channel, the estimated uncertainties in the pdf's in the high reconstructed mass region are $\pm 1.5\%$ for the signal, and ± 10–20% for the main background processes, $\mathrm{e^+e^-}\rightarrow \mathrm{q\bar{q}}$, WW and ZZ. The reconstructed mass pdf's were altered by $\pm 1\sigma$ of these estimated uncertainties. This alteration of the pdf's was applied to the $3\,\mathrm{GeV}/c^2$-wide region leading up to the kinematic threshold $M_{\mathrm{rec}} = \sqrt{s} - m_{\mathrm{Z}}$, where the most significant candidates are observed. Similarly, the reconstructed mass pdf's in the $\mathrm{h}\ell^+\ell^-$ and $\tau^+\tau^-\mathrm{q\bar{q}}$ channels were locally altered according to their estimated uncertainty in the region $M_{\mathrm{rec}} = 116 \pm 2\,\mathrm{GeV}/c^2$.

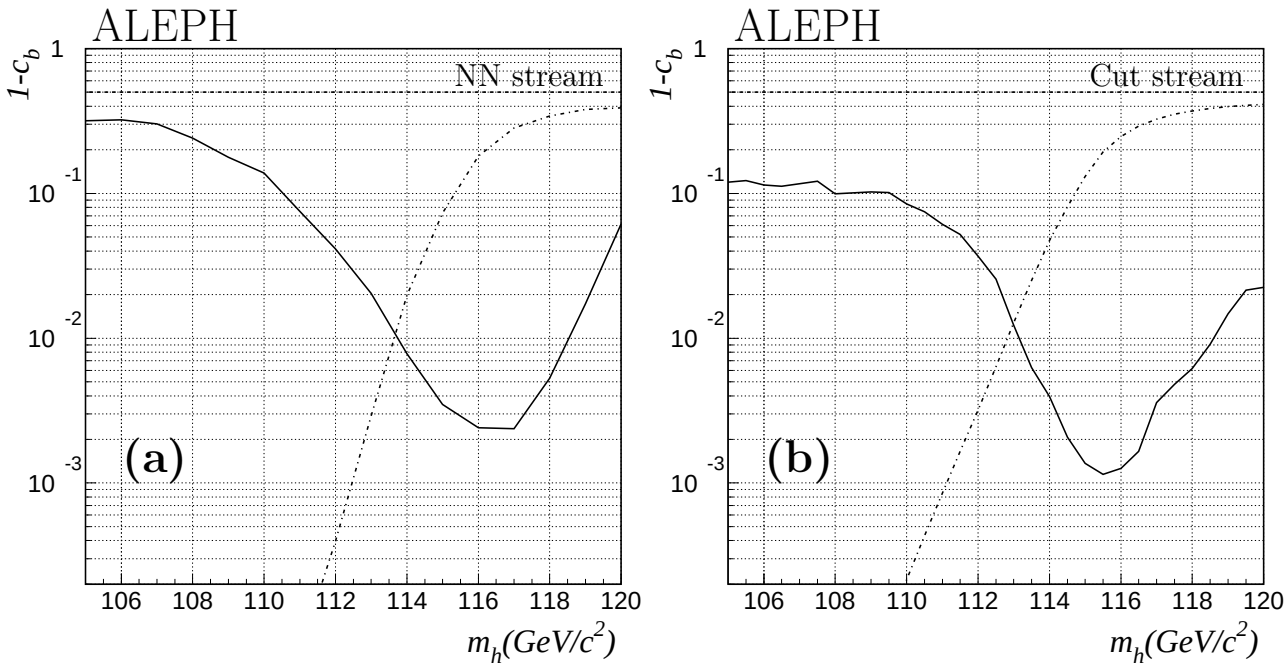

Figure 3: The observed (solid curve) and expected confidence levels for the background-only (dashed curve) and the signal (dash-dotted curve) hypotheses as a function of the Higgs boson test mass for (a) the NN stream and (b) the cut stream.

2. **Tagging of b jets**
   It has been determined [6, 13] that the track impact parameter resolution is 5–10% better in the simulation than in the calibration data taken at dedicated runs at the Z peak. This is the main limitation of the simulation of the most relevant b-tagging distributions. The agreement between data and simulation is restored by smearing the track parameters in the simulation.

   The smearing effectively results in correcting the signal and background event selection efficiencies. The systematic uncertainty on the efficiencies was estimated to be half the size of the correction. The event selection efficiencies were therefore varied accordingly, under the assumption that the b-rich processes (e.g., hZ, ZZ, Ze^+e^-) are fully correlated.

3. **Gluon splitting**
   The rate of gluon splitting to $b\bar{b}$ and $c\bar{c}$ quark pairs is underestimated in the simulation of the $e^+e^- \rightarrow q\bar{q}$ background. The measured splitting rates [14] are enforced by reweighting the four-jet events in the simulation that include a $g \rightarrow b\bar{b}$ or $g \rightarrow c\bar{c}$ branching. Twice the uncertainty of these measurements was conservatively propagated to the observed significance.

4. **Jet energy and angle resolutions**
   Small differences in the jet energy resolution and jet energy scale are observed when comparing the data and the simulation. The jet angular resolutions are also found to be slightly better in the simulation.

   The jets in the simulation were corrected [6] to improve the agreement between the

simulation and the data, and a systematic uncertainty amounting to half the size of the correction to the event selection efficiencies was assumed.

5. **Simulation of other selection variables**
   The systematic effects potentially originating from event selection variables other than those related to b tagging were evaluated with an event reweighting method [15]. For each variable the event weights were determined by making the simulated distribution agree with that in the data at a preselection level, i.e., with ample statistics. The effect of this reweighting on the selection efficiencies was assumed to be due to a possible systematic effect. Only small corrections, often statistically insignificant, were found and their magnitude added in quadrature for all variables.

6. **Strong coupling constant**
   A $\pm 5\%$ uncertainty on the strong coupling constant α_S was propagated to the $e^+e^- \to q\bar{q}$ background.

Table 5: Variation in the significance of the observed excess in the two analysis streams, at $m_h = 116\,\mathrm{GeV}/c^2$, due to the various systematic error sources.

Systematic source	Cut stream	NN stream
Simulated statistics:		
- $\tau^+\tau^- q\bar{q}$	$\pm 0.04\sigma$	$\pm 0.02\sigma$
- $h\ell^+\ell^-$	$\pm 0.02\sigma$	$\pm 0.02\sigma$
- $hq\bar{q}$	$\pm 0.11\sigma$	$\pm 0.07\sigma$
Tagging of b jets	$\pm 0.06\sigma$	$\pm 0.08\sigma$
Gluon splitting	$\pm 0.04\sigma$	$\pm 0.04\sigma$
Jet resolutions	$\pm 0.07\sigma$	$\pm 0.05\sigma$
Selection variables:		
- $h\ell^+\ell^-$	$\pm 0.03\sigma$	$\pm 0.03\sigma$
- $hq\bar{q}$	$\pm 0.03\sigma$	$\pm 0.05\sigma$
α_S	$\pm 0.04\sigma$	$\pm 0.06\sigma$

When all the uncertainties on the observed significance are added in quadrature, the total systematic uncertainty is found to be $\pm 0.17\sigma$ for the cut stream and $\pm 0.15\sigma$ for the NN stream.

6 Results in the context of the MSSM

In the MSSM, both the Higgstrahlung processes $e^+e^- \to hZ$, with a cross section proportional to $\sin^2(\beta-\alpha)$, and the associated pair production $e^+e^- \to hA$, with a cross section proportional to $\cos^2(\beta-\alpha)$, are searched for. Here, $\tan\beta$ is the ratio of the

vacuum expectation values of the two Higgs doublets and α is the Higgs mixing angle in the CP-even sector. As in the case of the SM Higgs boson search, the search for the MSSM Higgs bosons was also performed with the two alternative analysis streams [7].

In the search for hA pair production, ten events were selected in the 2000 data in the $\mathrm{b\bar{b}b\bar{b}}$ channel, with 5.5 events expected from SM background processes. This slight excess of events is fully correlated with that observed in the four-jet channel of the Standard Model Higgs boson search. In the $\mathrm{b\bar{b}}\tau^+\tau^-$ channel, three events were selected with 3.0 events expected.

The regions excluded at the 95% C.L. by the hZ and the hA searches independently, as well as by their combination, are shown in Fig. 4 as a function of $\sin^2(\beta-\alpha)$ with SM branching fractions assumed for the lighter CP-even Higgs boson h. The combined search allows an absolute lower limit on m_{h} of $89.8\,\mathrm{GeV}/c^2$ to be set at 95% C.L. These results are also interpreted in the context of two MSSM benchmark scenarios, called "no-mixing" scenario and "$m_{\mathrm{h}}^{\mathrm{max}}$" scenario, respectively [16]. The latter is expected to lead to rather conservative m_{h} and $\tan\beta$ exclusions, while the former is more favourable to LEP searches. The 95% C.L. excluded domains in the $(m_{\mathrm{h}}, \tan\beta)$ plane are shown for these two benchmark scenarios in Fig. 5, with $m_{\mathrm{top}} = 175\,\mathrm{GeV}/c^2$. The overall limits on m_{h}, m_{A} and $\tan\beta$ are summarized in Table 6.

Table 6: The excluded values (95% C.L.) of m_{h}, m_{A} and $\tan\beta$ in the two MSSM benchmark scenarios described in the text. The numbers in parentheses are the expected limits. The results are shown for the two alternative analysis streams.

	NN stream		Cut stream	
	No mixing	m_h^{max}	No mixing	m_h^{max}
$m_{\mathrm{h}} <$ (GeV/c^2)	89.8 (91.3)	89.8 (91.3)	89.8 (90.8)	89.8 (90.8)
$m_{\mathrm{A}} <$ (GeV/c^2)	90.1 (91.6)	90.1 (91.6)	90.1 (91.3)	90.1 (91.1)
$\tan\beta$	[0.5–6.2]	[0.7–2.3]	[0.5–5.0]	[0.7–2.2]

The theoretical upper limit on m_{h} for a given $\tan\beta$ (Figs. 5a, 5b) depends on m_{top}. For $m_{\mathrm{top}} = 180\,\mathrm{GeV}/c^2$, the excluded $\tan\beta$ range is significantly reduced to [0.8, 1.8] in the m_h^{max} scenario and to [0.5, 4.4] in the no-mixing scenario. The limits on m_{h} and m_{A} are not affected.

7 Invisible Higgs boson search results

In models which allow the Higgs boson to decay invisibly, the Higgstrahlung process gives rise to observable final states with acoplanar lepton pairs ($\mathrm{Z}\to\ell^+\ell^-$) and with acoplanar jets ($\mathrm{Z}\to\mathrm{q\bar{q}}$). An update of the searches [7, 8] for these two topologies is presented in this section, with the data collected in 2000.

The search for two acoplanar leptons was left unchanged; seven events were selected, in agreement with 6.7 events expected from background processes.

In the hadronic final state, the preselection was tightened to improve the rejection of Weν events. The energy of the less energetic hemisphere, formerly required to be

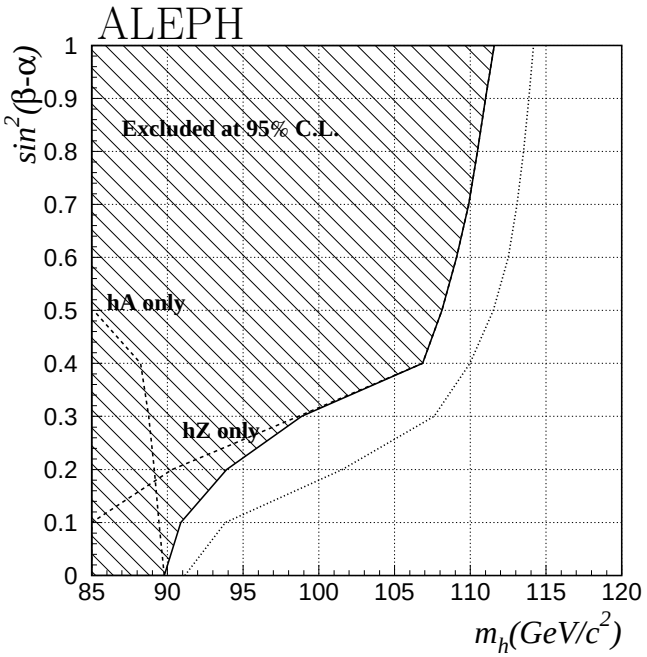

Figure 4: The 95% C.L. exclusion contours for the hZ and hA searches as a function of $\sin^2(\beta-\alpha)$ (dashed lines). The combined exclusion is shown by the hatched area and the dotted line indicates the expected exclusion.

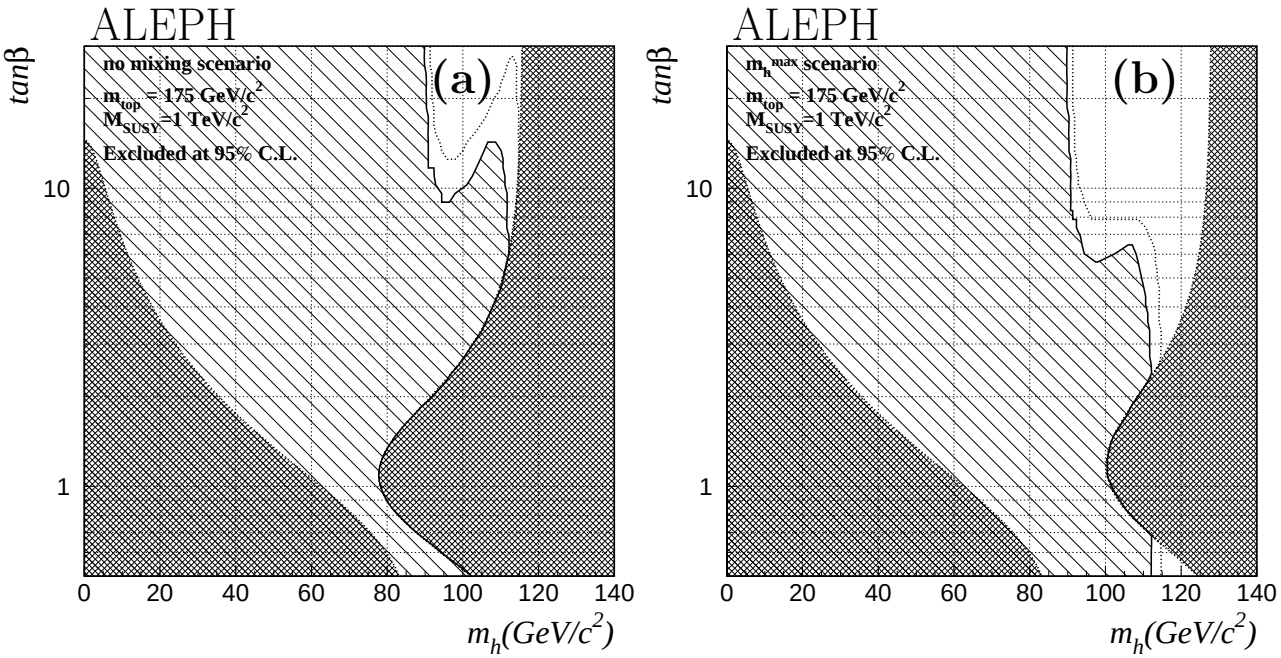

Figure 5: The experimentally excluded regions, at 95% C.L., in the $(m_{\rm h}, \tan\beta)$ parameter space, for (a) the no-mixing and (b) the $m_h^{\rm max}$ benchmark scenarios. The lightly-hatched area is excluded experimentally. The dotted line indicates the expected exclusion limit.The dark-hatched areas indicate theoretically forbidden parts of the parameter space.

nonzero [8], is now required to exceed 5% of the centre-of-mass energy. The data taken in 1999 [7] were studied with a set of three NN-based analyses, with the selection cut sliding as a function of the Higgs boson mass hypothesis. Each neural network was optimized for a given centre-of-mass energy (196, 200 or 202 GeV). If the distance to threshold $\sqrt{s} - m_{\mathrm{h}} - m_{\mathrm{Z}}$ is used as the sliding parameter rather than the Higgs boson mass hypothesis, m_{h}, the networks need neither be re-trained nor re-optimized. The same analysis can hence be applied to the numerous centre-of-mass energies scanned in the year 2000 with nearly optimal neural network trainings and selection criteria at each mass hypothesis. Altogether, 42 events were selected in the data, compatible with the 48.6 events expected from background processes.

These results are interpreted as a lower limit on m_{h} as a function of ξ^2, the product of the invisible branching fraction of the Higgs boson and a model-dependent factor which reduces the Higgstrahlung cross section with respect to that in the Standard Model (Fig. 6). For $\xi^2 = 1$, the observed mass lower limit is 114.1 GeV/c^2, for an expected 95% C.L. lower limit of 112.6 GeV/c^2.

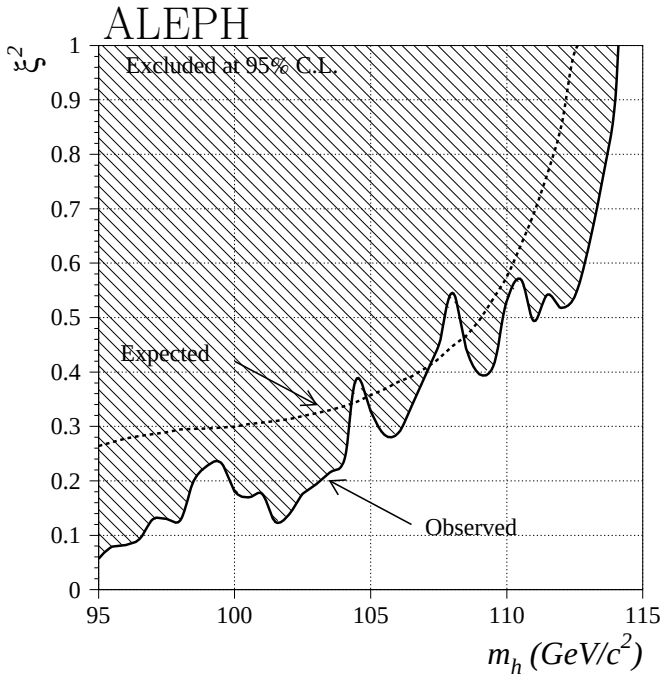

Figure 6: Result of the search for an invisibly-decaying Higgs boson. The observed (solid curve) and expected (dashed curve) exclusion regions in the (m_{h}, ξ^2) plane.

8 Conclusion

The final results of the ALEPH search for the Standard Model Higgs boson have been presented and have been found to confirm the preliminary findings reported in the ALEPH publication [1] that appeared shortly after the closing down of LEP.

The analysis of all the data collected in the year 2000 up to centre-of-mass energies of 209 GeV has been conducted with two parallel analyses, a neural-network-based stream and a cut-based stream. Both streams have revealed an excess with $\sim 3\sigma$ significance, consistent with a Higgs signal around $115\,\mathrm{GeV}/c^2$. The probability that such an excess is due to a fluctuation of the background is 2.4×10^{-3} for the NN stream. Most of this effect arises in the four-jet search channel, as would be expected in the signal hypothesis. A detailed study of the most important systematic error sources has shown that the significance of the observed excess is robust. A 95% C.L. lower limit on m_{h} is set at $111.5\,\mathrm{GeV}/c^2$.

In the framework of the MSSM, the searches for the hZ and hA processes have allowed absolute lower limits of 89.8 and $90.1\,\mathrm{GeV}/c^2$ to be set at 95% C.L. on the h and A masses, and the range $0.7 < \tan\beta < 2.3$ to be excluded if $m_{\mathrm{top}} = 175\,\mathrm{GeV}/c^2$. The search for an invisibly decaying Higgs boson in hZ production has allowed a 95% C.L. lower limit on m_{h} to be set at $114.1\,\mathrm{GeV}/c^2$, for a cross section equal to that in the Standard Model and a 100% branching fraction to invisible decays.

Acknowledgements

We congratulate our colleagues from the accelerator divisions for the very successful running of LEP at high energies. Without the extraordinary achievement of operating LEP at energies much above the design value, these observations would not have been possible. We are indebted to the engineers and technicians in all our institutions for their contribution to the excellent performance of ALEPH. Those of us from non-member countries thank CERN for its hospitality.

References

[1] The ALEPH Collaboration, *Observation of an excess in the search for the Standard Model Higgs boson at ALEPH*, Phys. Lett. **B495** (2000) 1.

[2] P.W. Higgs, Phys. Lett. **12** (1964) 132; Phys. Rev. Lett. **13** (1964) 508; Phys. Rev. **145** (1966) 1156;
F. Englert and R. Brout, Phys. Rev. Lett. **13** (1964) 321;
G.S. Guralnik, C.R. Hagen, and T.W.B. Kibble, Phys. Rev. Lett. **13** (1964) 585;
T.W.B. Kibble, Phys. Rev. **155** (1967) 1554.

[3] The DELPHI Collaboration, *Search for the Standard Model Higgs boson at LEP in the year 2000*, Phys. Lett. **B499** (2001) 23.

[4] The OPAL Collaboration, *Search for the Standard Model Higgs boson in e^+e^- collisions at $\sqrt{s} \approx$ 192–209 GeV*, Phys. Lett. **B499** (2001) 38.

[5] The L3 Collaboration, *Standard Model Higgs boson with the L3 experiment at LEP*, Phys. Lett. **B517** (2001) 319.

[6] The ALEPH Collaboration, *Search for the neutral Higgs bosons of the Standard Model and the MSSM in e^+e^- collisions at $\sqrt{s}$ = 189 GeV*, Eur. Phys. J. **C17** (2000) 223.

[7] The ALEPH Collaboration, *Searches for neutral Higgs bosons in e^+e^- collisions at centre-of-mass energies from 192 to 202 GeV*, Phys. Lett. **B499** (2001) 53.

[8] The ALEPH Collaboration, *Search for an invisibly decaying Higgs boson in e^+e^- collisions at 189 GeV*, Phys. Lett. **B466** (1999) 50.

[9] see e.g., G. Cowan, *Statistical Data Analysis*, Oxford University Press, 1998.

[10] The LEP Energy Working Group, *Evaluation of the LEP centre-of-mass energy for data taken in 2000*, LEP Energy Group 01-01.

[11] The LEP working group for Higgs boson searches, with the ALEPH, DELPHI, L3 and OPAL Colls., *Search for the Standard Model Higgs boson at LEP*, CERN-EP/2001-055 (July 2001).

[12] R.D. Cousins and V.L. Highland, *Incorporating systematic uncertainties into an upper limit*, Nucl. Instrum. and Methods **A320** (1992) 331.

[13] The ALEPH Collaboration, *Search for the neutral Higgs bosons of the MSSM in e^+e^- collisions at $\sqrt{s}$ from 130 to 172 GeV,* Phys. Lett. **B412** (1997) 173.

[14] The LEP Heavy Flavour working group, *Input parameters for the LEP/SLD electroweak heavy flavour results for Summer 1998 conferences*, LEP-HF/98-01.

[15] The ALEPH Collaboration, *Search for the Standard Model Higgs boson at the LEP2 collider near $\sqrt{s}$ = 183 GeV*, Phys. Lett. **B447** (1999) 336.

[16] M. Carena, S. Heinemeyer, C.E.M. Wagner and G. Weiglein, *Suggestions for improved benchmark scenarios for Higgs boson searches at LEP2*, CERN-TH/99-374 (1999).